THE JOURNAL OF PHYSICAL CHEMISTRY B

Article

pubs.acs.org/JPCB

Synthesis and Photophysical Properties of a Supramolecular Host–Guest Assembly Constructed by Fullerenes and Tryptamine Modified Hypocrellin

Zhize Ou,*[,†] Helin Jin,[†] Yunyan Gao,*[,†] Shayu Li,[‡] Haixia Li,[†] Yi Li,[§] Xuesong Wang,[§] and Guoqiang Yang[‡]

[†]Department of Applied Chemistry, School of Science, Northwestern Polytechnical University, Xi'an, 710072, People's Republic of China

[‡]CAS Key laboratory of Photochemistry, Institute of Chemistry, Chinese Academy of Sciences, Beijing 100190, People's Republic of China

[§]Technical Institute of Physics and Chemistry, Chinese Academy of Sciences, Beijing, 100190, People's Republic of China

Supporting Information

ABSTRACT: The metal coordination polymer of hypocrellin A bearing tryptamine motif (M–DTrpHA) can include fullerene via a two-point interaction, involving $\pi-\pi$ stacking and electron donor–acceptor interaction. The 1:1 host–guest system M–DTrpHA/fullerene exhibits a moderate association constant K_a (6.62×10^4 to 6.46×10^5 M^{-1}). Both of the metal ions in M–DTrpHA and the substituents connected to the fullerene core play important roles in stabilizing the M–DTrpHA/fullerene complex. Transient absorption spectral and NIR absorption spectral results demonstrate that, in the M–DTrpHA/fullerene system, efficient photoinduced electron transfer from the tryptamine group in M–DTrpHA to fullerene may occur, resulting in a long-lived fullerene anion radical. The observed order of quantum yield (Φ_{ET}^{T}) and rate constants (K_{ET}^{T}) for electron transfer via $^3C_{60}$* is Y^{3+}–DTrpHA > La^{3+}–DTrpHA > DTrpHA, consistent with their binding ability to C_{60}. The nanostructure of M–DTrpHA is rearranged to form an interpenetrating network after interaction with fullerene.

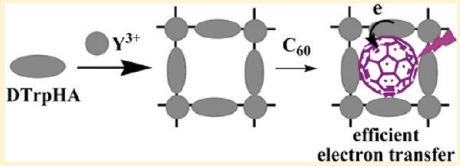

INTRODUCTION

Coordination polymers have received growing interest due to their structural diversities and potential applications in smart optoelectronic, magnetic, catalytic, and biological materials.[1] Depending on the flexibility and preferred conformation of the bridging ligands, coordination polymers can form oligomers[2] and rigid[3] and flexible porous frameworks.[4] Incorporation of redox-active and/or photoactive guest molecules into the nano-sized space of a coordination polymer can provide an opportunity for studying the fundamental physical properties of assemblies in confined nanospaces,[5] and may be one of the strategies to mimic the efficient energy/electron transfer processes in natural energy conversion systems.[6] The well-designed structures of coordination polymers are aprerequisite for efficient accommodation of specific guest molecules and are important to develop novel multifunctional materials.[7] Introduction of aromatic fragments into ligands is one way to enhance the interaction between polymer and guest molecules through $\pi-\pi$ stacking, CH–π, and hydrophobic interactions.[8]

Fullerene is widely used as an electron acceptor in organic solar cells, photovoltaic devices, and biochemistry, due to its low reduction potentials and small reorganization energy.[9] Many efforts have been taken to incorporate fullerenes into highly organized supramolecular arrays,[10] in order to get well-defined nanoscopic architectures with long-lived charge-separated states and to modulate the spatiotemporal arrangement of electroactive entities.[11] To achieve this objective, a broad variety of fullerene receptors have been explored, including derivatives of calix[n]-arenes,[12] cyclotriveratrylenes,[13] cycloparaphenylene,[14] π-extended tetrathiafulvalenes,[15] and, most frequently, self-assembly of porphyrin arrays.[16] Recently, coordination cages bearing large aromatic panels and metal ions appear as novel molecular receptors for fullerenes.[17] The coordination polymers, possessing a suitable cavity and sufficient flexibility, have been engineered to capture fullerenes.[18] The chemical structure of fullerene plays a critical role in regulating the binding constant of the supramolecular assembly.[19] However, these supramulecular assemblies constructed by coordination polymers and fullerenes show limited solution-based behavior, which may hinder their further applications.

Recently, our results demonstrate that hypocrellin, a type of naturally occurring perylenequinonoid, can act as a receptor for the fullerenes.[20] The supramolecular assembly can be formed by the magnesium coordination polymer of hypocrellin A (Mg^{2+}–HA) and C_{60} in both solution and solid state.[21] The efficiency of electron transfer from electron donor to fullerene is improved by employing Mg^{2+}–HA as an electron mediator. When the extra donor *N*,*N*′-dimethylaniline is added, the electron paramagnetic resonance (EPR) signal intensity of $C_{60}^{\bullet-}$ in Mg^{2+}–HA/C_{60}

Received: October 17, 2011
Revised: January 8, 2012
Published: January 18, 2012

   dx.doi.org/10.1021/jp209969f | *J. Phys. Chem. B* 2012, 116, 2048–2058

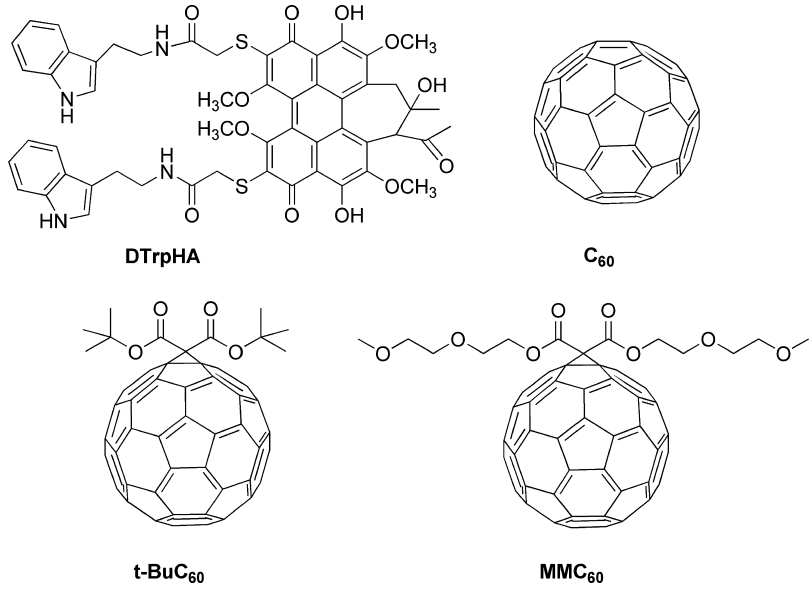

Figure 1. Chemical structure of DTrpHA and fullerene derivatives.

increases 9-fold as strong as that in the absence of Mg^{2+}–HA. Tryptamine, a biogenic amine, plays a role as a neuromodulator or neurotransmitter in mammals.[22] It can also act as an electron donor and be oxidized via photoinduced electron transfer from tryptamine to dye triplet.[23] Herein, tryptamine linked HA (DTrpHA) is synthesized. The electron transfer processes in a supramolecular assembly involving a coordination polymer of DTrpHA and fullerene are investigated in detail, which may be helpful for extending the application of the hypocrellin/fullrene system. The rare earth ions, Y^{3+} and La^{3+}, are chosen to chelate with DTrpHA to form a coordination polymer due to their high affinity to hypocrellin A[24] and potential elongating lifetime of the charge-separated state in the quinone dyad.[25] Fullerene derivatives with different substituents (Figure 1) are incorporated into these polymers by a two-point binding strategy: $\pi-\pi$ stacking interaction (aromatic ring of hypocrellin–fullerene) and electron donor–acceptor interaction (conjugated tryptamine–fullerene).[26] The binding behavior and photoinduced electron-transfer processes in the M–DTrpHA/fullerene system are investigated using UV–vis spectroscopy, fluorescence spectroscopy, nanosecond transient absorption measurements, and transmission electron microscopy (TEM).

EXPERIMENTAL METHODS

Chemicals. Hypocrellin A (HA) was isolated from the fungus sacs of *Hypocrella bambusae* and recrystallized twice from acetone before use. DTrpHA and fullerene derivatives were synthesized in our laboratory (see details in the Supporting Information). *N*,*N*′-Dimethyl formamide (DMF), dimethyl sulfoxide (DMSO), tryptamine, mercaptoacetic acid, $YCl_3{\cdot}6H_2O$, and $LaCl_3{\cdot}7H_2O$ were purchased from Acros Organics. Fullerene C_{60}, 4-dimethylaminopyridine (DMAP), *N*,*N*′-dicyclohexyl carbodiimide (DCC), *n*-tetrabutylammonium perchlorate, and 1-hydroxybenzotriazole hydrate (HOBT) were purchased from Sigma-Aldrich Company. DMF and DMSO were dried over CaH_2 and distilled prior to use. Anhydrous ethanol and other chemicals of analytical grade were obtained from Beijing Chemical Plant.

Measurements of Spectral and Electrochemical Properties. Steady state absorption and fluorescence spectra were recorded with a Hitachi UV-3010 UV–vis spectrophotometer, Perkin-Elmer Lambda 950 UV/vis/NIR spectrophotometer, and Hitachi F-4600 spectrofluorimeter, respectively. The fluorescence experiments were carried out in a 5 mm × 5 mm cuvette, and DTrpHA was selectively excited at 295 nm.

Nanosecond transient absorption spectra were performed on a LP-920 pump–probe spectroscopic setup (Edinburgh). The excited source was the unfocused second harmonic (532 nm) output of a Nd:YAG laser (Continuum surelite II); the probe light source was a pulse-xenon lamp. The signals were detected by Edinburgh analytical instruments (LP900) and recorded on a Tektronix TDS 3012B oscilloscope and a computer.[27] A liquid-nitrogen-cooled germanium (Ge) detector was used to monitor the emission signal in the NIR range.[28]

Cyclic voltammetry (CV) experiments were performed on a CHI660D electrochemical workstation by a cyclic voltammetry (CV) technique in DMSO–toluene (4/1, v/v) solution, using two platinum wires as the working and counter electrodes, respectively, and a saturated calomel electrode (SCE) as the reference electrode in the presence of 1 mM *n*-tetrabutylammonium perchlorate as the supporting electrolyte.[29]

UV–vis Job's Plot of M–DTrpHA with Fullerenes. Stock solutions of M–DTrpHA (40 μM) and fullerenes (40 μM) were prepared, and solutions with a molar fraction of M–DTrpHA from 0.1 to 0.9 were prepared in 5 mL volumetric flasks by diluting the required amount of the stock solutions. The total concentration of M–DTrpHA and fullerenes was fixed at 40 μM. The vertical coordination (ΔA) in differential absorption spectra represented the difference between the absorption of the mixed solution and that of the neat fullerenes and M–DTrpHA solutions at corresponding concentrations.[30]

Fluorescence Titration. The titrations were performed by adding the required volumes of a solution of fullerene (1 mM) into the solution of M–DTrpHA (10 μM). Under experimental conditions, the fluorescence of M–DTrpHA decreased with

dx.doi.org/10.1021/jp209969f | J. Phys. Chem. B 2012, 116, 2048–2058

increasing fullerene concentration. According to eq 1,

$$\text{M}-\text{DTrpHA} + \text{C}_{60} \overset{K_a}{\rightarrow} \text{M}-\text{DTrpHA}/\text{C}_{60} \quad (1)$$

The association constant (K_a) of the formed M−DTrpHA/C_{60} complex could be determined using the nonlinear least-squares method according to the curve fitting in eq 2[31]

$$\Delta F = F_0 - F = \{\alpha([\text{M}-\text{DTrPHA}] + [\text{C}_{60}] + 1/K_a) - \sqrt{\alpha^2([\text{M}-\text{DTrPHA}] + [\text{C}_{60}] + 1/K_a)^2 - 4\alpha^2[\text{M}-\text{DTrPHA}]\cdot[\text{C}_{60}]}\}/2 \quad (2)$$

where F_0 and F were the fluorescence of M−DTrpHA at the given wavelength in the absence and presence of C_{60} and α was the proportionality coefficient, which may be taken as a sensitivity factor for the fluorescence change induced by the addition of one molar guest.

RESULTS AND DISCUSSION

Complexation of DTrpHA with Metal Ions. Photoreaction with mercaptoacetic acid is one of the important approaches to synthesize hypocrellin derivatives.[32] It is necessary to optimize the concentration of O_2 to achieve high yield. In our experiment, air is bubbled into the reaction system at a rate of 10 mL·min^{-1} and the reaction solution is stirred vigorously (>600 rpm) to enhance the diffusion of oxygen. The 5,8-di-(mercaptoacetic acid)−HA is obtained as the main product, and the collection yield is up to 56%. Subsequently, the typical electron donor tryptamine[33] is covalently linked to 5,8-di-(mercaptoacetic acid)−HA through amidation reaction, affording tryptamine modified HA (DTrpHA).

It has been reported that HA itself can form stable complexes with rare earth trivalent ions.[24] In this work, the interaction of DTrpHA with rare earth trivalent ions Y^{3+} and La^{3+} is investigated using UV−vis absorption spectroscopy. In ethanol solution, DTrpHA exhibits two absorption peaks at 267 and 514 nm and a shoulder peak at 599 nm, respectively. Upon addition of Y^{3+}, these peaks are red-shifted to 285, 557, and 610 nm, respectively, with a new peak appearing at 655 nm (Figure 2). Remarkable changes in the absorption spectra indicate that Y^{3+} can strongly chelate with DTrpHA. During the entire titration processes, one set of isosbestic points at 276, 408, and 537 nm is observed within the spectral region (250−750 nm) under study, indicating that only one form of complex is produced in the system.

The stoichiometry of the complexes is determined by both the molar ratio and the continuous variation methods.[34] For the molar ratio method, a series of ethanol solutions is prepared in which the concentration of DTrpHA is held constant (20 μM), while that of the Y^{3+} is varied. The absorbance at 655 nm is plotted against the molar ratio of $[Y^{3+}]/[\text{DTrpHA}]$ (Figure 2a, inset). Two straight lines of different slopes can be derived from the plot, and the extrapolated intersection occurs at a mole ratio of 1:2, corresponding to the ratio of Y^{3+} to DTrpHA in the complex. For the continuous variation method, the total concentration of Y^{3+} and DTrpHA is kept constant (40 μM), while the molar fractions of Y^{3+} in the mixed solutions continuously varied. The absorbance differences (ΔA) between the mixed solutions and the neat DTrpHA solution are plotted against the molar fraction of DTrpHA. As shown in Figure 2b, the maximum ΔA occurs at the molar fraction of 0.66, supporting the 1:2 molar ratio of Y^{3+} and DTrpHA in the complex, too.

Similarly, upon addition of La^{3+}, the absorption peaks of DTrpHA shift from 514, 599 nm to 550, 609 nm in the visible region, respectively, and a new peak appears at 663 nm (Figure 3).

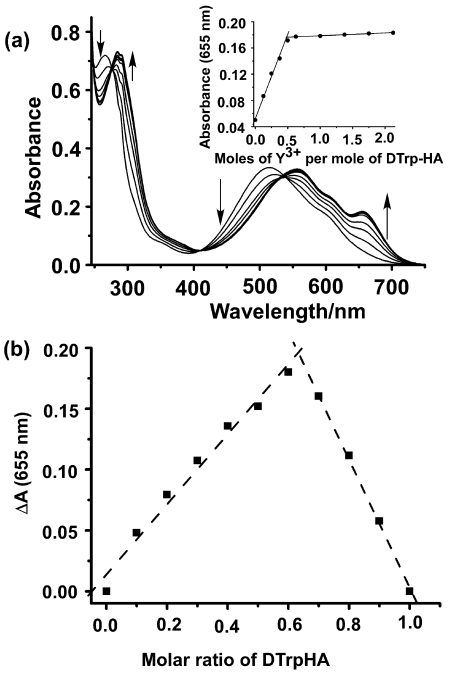

Figure 2. (a) Absorption spectra of DTrpHA in ethanol upon addition of Y^{3+}. [DTrpHA] = 20 μM. $[Y^{3+}]$ = 0, 2.5, 5, 7.5, 10, 12.5, 20, 27.5, 35, and 42.5 μM. (b) Job's plot for the Y^{3+}−DTrpHA in ethanol obtained by plotting the absorbance differences (ΔA) at 655 nm ($[\text{DTrpHA}] + [Y^{3+}]$ = 40 μM). Inset: Molar ratio plot for Y^{3+}−DTrpHA obtained by plotting the absorbance at 655 nm as a function of the molar ratio of Y^{3+} to DTrpHA.

The experimental results of both the molar ratio method and the continuous variation method suggest that La^{3+} may form a complex with DTrpHA with a molar ratio of 1:2 ($[La^{3+}]/[\text{DTrpHA}]$).

Complexation also gives rise to significant changes in IR and ^{1}H NMR spectra of DTrpHA. DTrpHA exhibits a sharp IR absorption around 1654 cm^{-1}, which is attributed to the stretching vibration of the quinonoid carbonyl groups. In the complexes, this band shifts to a lower frequency of 1637 cm^{-1}, indicating the participation of the quinonoid carbonyl group in coordination.[35] The ^{1}H NMR signal of the phenolic hydroxyl group of DTrpHA shifts downfield to 18.2 on complexation, suggesting their participation in coordination. Furthermore, a broad IR absorption band around 500−750 cm^{-1} appearing in

dx.doi.org/10.1021/jp209969f | J. Phys. Chem. B 2012, 116, 2048−2058

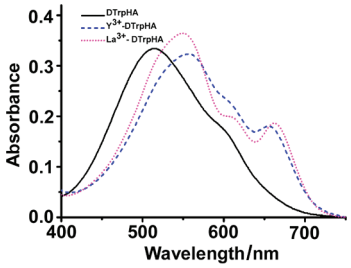

Figure 3. Absorption spectra of DTrpHA (solid line), Y^{3+}–DTrpHA (dashed line), and La^{3+}–DTrpHA (dotted line) in ethanol.

the complex may be attributed to a meta-O band. Addition of $AgNO_3$ to the aqueous solution of Y^{3+}–DTrpHA leads to the precipitation of AgCl, suggesting that Cl^- is the counterion in the complex. Owing to the use of a dialysis membrane (molecular weight cutoff of 5000) in the purification, the obtained M^{3+}–DTrpHA complexes should possess polymer-like structures.

Taking the fact that the coordination numbers of the Y^{3+} and La^{3+} can be up to eight in coordination polymer[36] and also taking all the above-mentioned findings into consideration, the structure of M–DTrpHA is proposed to be a 2-D coordination polymer (Figure 4). Y^{3+} and La^{3+} may complex with four

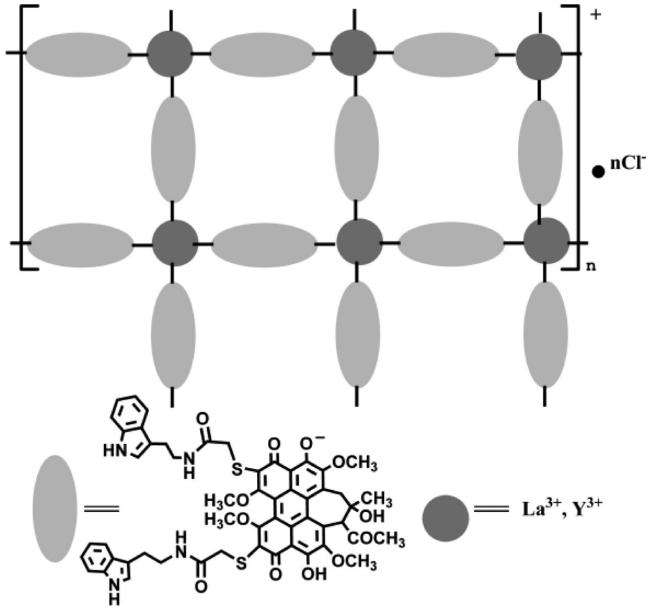

Figure 4. Proposed 2-D structure for DTrpHA complexes with Y^{3+} and La^{3+}.

quinonoid carbonyl oxygens and four phenolic oxygens. Similar results of a 1:2 ratio of metal ions with organic molecules forming a 2-D coordination polymer have also been reported previously.[37]

Electrochemical Measurements. Hypocrellin and fullerene are two excellent electron acceptors. Photoinduced electron transfer reactions involving hypocrellin and fullerene predominantly proceed through their triplet excited states, due to their high triplet quantum yields.[38] Cyclic voltammetric studies are performed to visualize the redox state and to evaluate the energetics of the electron transfer reaction. The reduction potentials of Y^{3+}–DTrpHA and La^{3+}–DTrpHA are more positive than that of DTrpHA (Table 1), which can be attributed to the association of metal ions with the anion radical of

Table 1. Redox Potentials of Model Compounds and the Calculated Results of the Free Energy Changes of Photoinduced Electron Transfer Reactions in the M–DTrpHA/Fullerene Complex

			ΔG (eV)	
compounds	E_{red} (V vs SCE)	E_{ox} (V vs SCE)	M–$DTrp^{\bullet+}HA^{\bullet-}$ [a]	Y^{3+}–$DTrp^{\bullet+}HA/C_{60}^{\bullet-}$ [b]
DTrpHA	−0.98	0.82	−0.10	
Y^{3+}–DTrpHA	−0.86	0.82	−0.22	
La^{3+}–DTrpHA	−0.89	0.82	−0.19	
C_{60}	−0.54			−0.20
MMC_{60}	−0.64			−0.10
t-$BuMC_{60}$	−0.65			−0.09

[a] ΔG for intramolecular electron transfer between hypocrellin and tryptamine units in M–DTrpHA. [b] ΔG for intermolecular electron transfer between tryptamine units in Y^{3+}–DTrpHA and fullerenes.

DTrpHA.[27,39] The oxidation potential of the tryptamine group is measured to be 0.82 V versus SCE. The intramolecular electron transfer from ground state tryptamine to triplet state DTrpHA and M–DTrpHA is a thermodynamically favorable process ($\Delta G < 0$) (Table 1), estimated by the Rehm–Weller equation (eq 3)[40]

$$\Delta G = E_{ox}(\text{donor}) - E_{red}(\text{acceptor}) - E_T(\text{excited state energy}) - C \quad (3)$$

where E_{ox}(donor) is the oxidation potential of the donor, E_{red}(acceptor) is the reduction potential of the acceptor, E_T is the triplet excited energy of DTrpHA and M–DTrpHA assumed to be similar to that of HA (1.84 eV),[36] and C is the static Coulomb energy of $D^{\bullet+}$–$A^{\bullet-}$ (can usually be regarded as 0.06 eV in polar solvents).

MMC_{60} and *t*-BuC_{60} exhibit a more negative value of the first reduction potential than that of pristine C_{60} as a consequence of the partial loss of π-conjugation.[41] The intermolecular electron transfer from the tryptamine moiety in M–DTrpHA to fullerenes is a thermodynamically favorable process ($\Delta G < 0$) (Table 1), calculated by the Rehm–Weller equation (eq 3), where the triplet excited energy of fullerenes is assumed to be 1.50 eV.[42] The strong electron donor–acceptor interaction between tryptamine and fullerenes may facilitate the inclusion of fullerene into cavities in M–DTrpHA.[43]

Association of Fullerenes with M–DTrpHA in Solution. Introduction of fullerene into a preorganized system is one of the important ways to construct a supramolecular assembly.[44] Our previous results demonstrate that HA cannot form a stable complex with fullerene C_{60}, while the coordination polymer Mg^{2+}–HA can form a stable complex with C_{60} due to the synergy effect of the HA unit in the coordination polymer.[30,45] The interaction of fullerene with DTrpHA and its rare metal complexes is investigated by UV–vis absorption and fluorescence spectroscopy.

As shown in Figure 5a, addition of C_{60} leads to negligible changes of the absorption spectra of DTrpHA, suggesting weak interaction between DTrpHA and C_{60}. The peak at 407 nm is a characteristic absorption peak of C_{60}. When aliquots of C_{60}

dx.doi.org/10.1021/jp209969f | J. Phys. Chem. B 2012, 116, 2048–2058

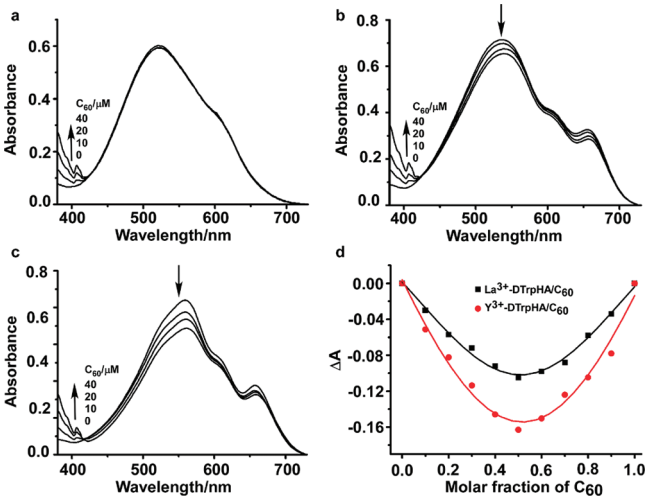

Figure 5. UV−vis spectral changes of (a) DTrpHA (40 μM), (b) La^{3+}−DTrpHA (20 μM), and (c) Y^{3+}−DTrpHA (20 μM) in the presence of C_{60} in DMSO−toluene solution (4/1, v/v). (d) Job's plot for the interaction between M−DTrpHA and C_{60} in DMSO−toluene solution (4/1, v/v). The Job's plot for Y^{3+}−DTrpHA and La^{3+}−DTrpHA is carried out using the difference in absorbance at 558 and 535 nm, respectively.

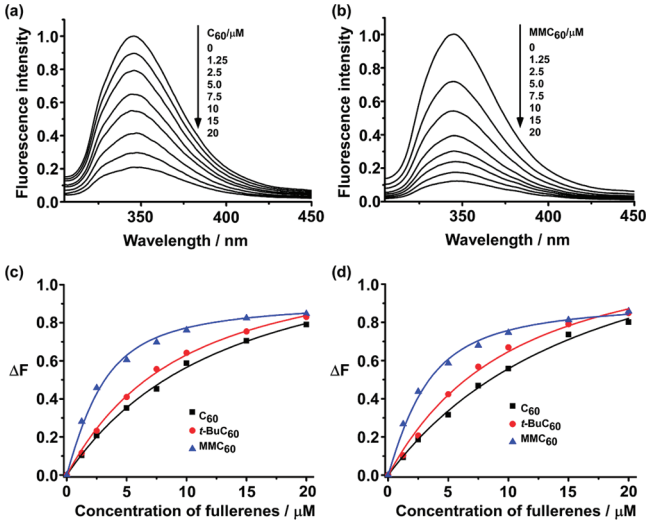

Figure 6. Fluorescence emission spectra of Y^{3+}−DTrpHA (2.5 μM) in DMSO−toluene solution (4/1, v/v) containing different concentrations of (a) C_{60} and (b) MMC_{60}. Differential fluorescence intensity of (c) Y^{3+}−DTrpHA and (d) La^{3+}−DTrpHA upon addition of fullerenes used to calculate K_a by nonlinear least-squares curve-fitting analysis.

solution are added into the solution of La^{3+}−DTrpHA, the absorption peak of La^{3+}−DTrpHA is red-shifted from 535 to 540 nm, and an isosbestic point at 428 nm appears (Figure 5b). Similarly, addition of C_{60} solution into the solution of Y^{3+}−DTrpHA also brings about a red-shift of the absorption peak from 558 to 562 nm, with an isosbestic point at 416 nm (Figure 5c). These results indicate that C_{60} can associate with La^{3+}−DTrpHA and Y^{3+}−DTrpHA. As shown in Figure 5d, the minimum ΔA occurs at a molar fraction of 0.5 in the Job's plot, suggesting a 1:1 molar ratio of C_{60} to M−DTrpHA in supramolecular assemblies.

Along with the UV−vis spectral changes, a decrease in the fluorescence intensity of Y^{3+}−DTrpHA at 346 nm (assigned to the tryptamine moiety) is also observed upon addition of C_{60} or MMC_{60} (Figure 6a and b). The fluorescence intensity of tryptamine in DTrpHA or M−DTrpHA is much lower than that of free tryptamine, which can be attributed to the electron transfer from the singlet excited state tryptamine to the hypocrellin group (Figure S4, Supporting Information).[46] The fluorescence at 346 nm of the tryptamine moiety in Y^{3+}−DTrpHA is further quenched by C_{60} molecules, without the appearance of the fluorescence of C_{60} at 700 nm, suggesting that the electron transfer, rather than energy transfer, is the main pathway for fluorescence quenching by C_{60} molecules.[47] The binding constants (K_a) between M−DTrpHA and fullerenes are calculated by analyzing the sequential changes in fluorescence intensity (ΔF) of M−DTrpHA at varying concentrations of fullerenes using a nonlinear least-squares curve-fitting method (Figure 6c and d). For each host M−DTrpHA examined, the plot of ΔF as a function of fullerene concentration gives an excellent fit ($R^2 > 0.994$), verifying the validity of the 1:1 complex stoichiometry assumed above, which is consistent with the UV−vis spectral results (Figure 5). The association constants K_a between M−DTrpHA and fullerenes are summarized in Table 2.

The association constants K_a are in the range between 6.62×10^4 and 6.46×10^5 M^{-1}, similar to the values for the complexation of C_{60} with porphyrin.[48] The nature of capturing fullerene to La^{3+}−DTrpHA or Y^{3+}−DTrpHA may be due to π−π stacking interactions between HA groups and C_{60}, like the case of the noncovalent binding of fullerenes by aromatic components such as porphyrins and calixarenes.[49] The electron donor−acceptor interaction between tryptamine in M−DTrpHA and fullerene may further stabilize the M−DTrpHA/fullerene complex.[43]

The association constants of the M−DTrpHA/fullerene complexes are strongly dependent on the substituents connected to the fullerene core. With receptor Y^{3+}−DTrpHA, the K_a value increased from 8.79×10^4 M^{-1} for C_{60} to 1.30×10^5 M^{-1} for t-BuC_{60} and to 6.46×10^5 M^{-1} for MMC_{60}. MMC_{60} and t-BuC_{60} possess a higher solubility than C_{60} in DMSO−toluene solution, which may reduce the known fullrene−fullerene attraction forces and consequently construct a more stable fullerene supramolecular assembly.[50] Considering that lanthanide ions possess a large coordination number (in the range of 6−12) on formation of a complex, the lanthanide ion (Y^{3+} and La^{3+}) in M−DTrpHA may chelate with the ether oxygen groups in the ethyleneglycol chain of MMC_{60} to saturate the coordination number.[51] As a result, the association constant of MMC_{60} is much higher than that of t-BuC_{60} or C_{60}, when complexing with M−DTrpHA.

Table 2 also shows Y^{3+}−DTrpHA has a higher affinity toward fullerenes than La^{3+}−DTrpHA. It has been reported that the minimum width of the channel of coordination polymer decreases in an approximately linear manner with the ion radius of the metal ion.[52] Considering that Y^{3+} ion has a smaller radius (88 pm) than that of La^{3+} (106 pm),[53] it can be reasonably deduced that the channel formed by Y^{3+}−DTrpHA is smaller than that of La^{3+}−DTrpHA. The subtle structural variation of the host molecules may have an effect on the binding abilities to guest fullerene.[15]

Nanosecond Transient Absorption Studies. Information on the excited-state interactions in M−DTrpHA/fullerene is obtained from transient absorption spectra in the visible regions. No transient absorption signal is observed when DTrpHA is irradiated with 532 nm laser. In contrast, when

dx.doi.org/10.1021/jp209969f | J. Phys. Chem. B 2012, 116, 2048−2058

Table 2. Association Constants (K_a) for the Complexation of Fullerene Derivatives with M−DTrpHA in DMSO−Toluene Solution

	C_{60}		*t*-BuC_{60}		MMC_{60}	
	K_a (M^{-1})	R^2	K_a (M^{-1})	R^2	K_a (M^{-1})	R^2
Y^{3+}−DTrpHA	8.79×10^4	0.9972	1.30×10^5	0.9947	6.46×10^5	0.9951
La^{3+}−DTrpHA	6.62×10^4	0.9982	1.18×10^5	0.9985	5.66×10^5	0.9942

Y^{3+}−DTrpHA or La^{3+}−DTrpHA is irradiated, transient absorption bands with maxima at 420, 590, and 710 nm and a minimum band at 520 and 660 nm can be observed (Figure S5, Supporting Information). In the presence of typical reductants, such as triethylamine and *N,N,N′,N′*-tetramethylethylene diamine (TEMED), the intensities of these bands increase. Thus, these bands can be assigned to the hypocrellin anion radical of M−DTrpHA$^{\bullet-}$. The decay curves for Y^{3+}−DTrpHA$^{\bullet-}$ and La^{3+}−DTrpHA$^{\bullet-}$ at 590 nm can be fitted monoexponentially with lifetimes of 14.2 and 8.31 μs, respectively.

After illuminating an argon-saturated DMSO−toluene solution of DTrpHA for 2 min with Nd:YAG laser (532 nm), an electron paramagnetic resonance (EPR) signal with a *g* value of 2.002 is recorded, which can be confirmed as the hypocrellin radical anion (Figure S6, Supporting Information).[32] This result suggests that photoinduced charge separation may take place (eq 4). However, the charge recombination may be very fast so that the lifetime of DTrp$^{\bullet+}$HA$^{\bullet-}$ is too short to be detected by nanosecond laser flash photolysis.[54] However, in M−DTrpHA, the charge recombination may be slowed down due to the Columbic attraction of electron on DTrpHA$^{\bullet-}$ with metal ions and the lifetime of DTrpHA$^{\bullet-}$ elongated, consistent with the literature.[25] The absorption band of the cation radical of tryptamine at 510 nm[55] is not observed, maybe due to its weak absorbance and overlap with the absorption of M−DTrpHA$^{\bullet-}$.

$$\text{DTrpHA} \xrightarrow{h\nu} \text{DTrp}^{\bullet+}\text{HA}^{\bullet-} \quad (4)$$

Figure 7a shows the transient absorption spectra of Y^{3+}−DTrpHA in the presence of C_{60}. The absorption band at 590 nm corresponds to the anion radical of Y^{3+}−DTrpHA$^{\bullet-}$ and the band at 750 nm to the triplet state of C_{60}.[56] With the decay of $^3C_{60}$ at 750 nm, the band at 1080 nm increases, which can be assigned to $C_{60}^{\bullet-}$.[57] The slow rise of the 1080 nm band in Figure 7 reaches a maximum at about 5 μs, indicating that the bimolecular collisional electron transfer via triplet states of M−DTrpHA and C_{60} and slow electron migration may occur. The first reduction potential of C_{60} is more positive than that of M−DTrpHA (Table 1), which suggests electron transfer from Y^{3+}−DTrpHA$^{\bullet-}$ to C_{60} is a thermodynamic favorable process.[20,30] The lifetimes of Y^{3+}−DTrpHA$^{\bullet-}$ in Y^{3+}−DTrpHA and La^{3+}−DTrpHA$^{\bullet-}$ in La^{3+}−DTrpHA only slightly decrease upon formation of a supramolecular assembly with fullerenes (Table S1, Supporting Information), indicating inefficient electron transfer from the hypocrellin anion radical in M−DTrpHA to fullerenes. The fullerene anion radical in the M−DTrpHA/fullerene system may mainly arise from photoinduced electron transfer from tryptamine to the triplet state of fullerene (eq 5), in agreement with the fluorescence quenching and electrochemical results. Fitting the decay dynamics of $C_{60}^{\bullet-}$ according to first-order kinetic analysis, the lifetime of $C_{60}^{\bullet-}$ is determined to be 17.0 μs in Y^{3+}−DTrpHA/C_{60} and 16.9 μs in the La^{3+}−DTrpHA/C_{60} system (Figure 7a, inset), respectively. The transient absorption of $^3C_{60}$* at 750 nm decays double exponentially with a longer lifetime of 29.7 μs and a shorter one of 6.67 μs when C_{60} is forming a complex with Y^{3+}−DTrpHA (Table S1, Supporting Information). The longer lifetime component can be assigned to the triplet state of pristine C_{60}, and the shorter one may be because of the interaction between M−DTrpHA and triplet C_{60}.

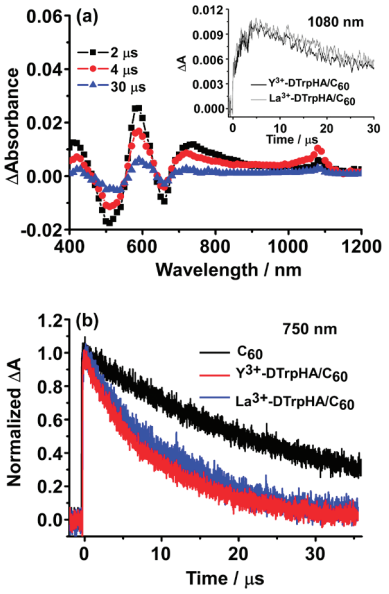

Figure 7. (a) Transient absorption spectra of Y^{3+}−DTrpHA/C_{60} observed by 532 nm laser irradiation in Ar-saturated DMSO−toluene (4/1, v/v). (b) Time profiles of the pristine C_{60}, Y^{3+}−DTrpHA/C_{60}, and La^{3+}−DTrpHA/C_{60} at 750 nm. Inset: Time profiles of Y^{3+}−DTrpHA/C_{60} and La^{3+}−DTrpHA/C_{60} at 1080 nm. [Y^{3+}−DtrpHA] = [La^{3+}−DtrpHA] = [C_{60}] = 40 μM.

$$Y^{3+}\text{−DTrpHA} + {}^3C_{60}^* \rightarrow Y^{3+}\text{−DTrp}^{\bullet+}\text{HA} + C_{60}^{\bullet-} \quad (5)$$

The decay rate of $^3C_{60}$* at 750 nm (Figure 8a) and the transient intensity of $C_{60}^{\bullet-}$ at 1080 nm (Figure 8b) increase with increasing concentration of Y^{3+}−DTrpHA. Immediately after the laser pulse, each absorbance intensity increases from absorbance = 0 at time = 0, which denies the contribution of the fast electron transfer processes from the singlet state (Figure 8b). These results further indicate that $^3C_{60}$* can be quenched by Y^{3+}−DTrpHA and $C_{60}^{\bullet-}$ is formed as a product of electron transfer (eq 5). Quenching rate constants (K_q^T) of $^3C_{60}$* are determined from the linear dependence of pseudo-first-order decay constants (K_{first}) on quencher concentration (Figure 8c).[58] The quantum yield of the electron transfer process (Φ_{ET}^T) via $^3C_{60}$* is calculated directly from the maximum $^3C_{60}$* absorption ($\Delta A_{^3C_{60}*}$) at 750 nm and $C_{60}^{\bullet-}$ absorption ($\Delta A_{C_{60}^{\bullet-}}$) at

dx.doi.org/10.1021/jp209969f | J. Phys. Chem. B 2012, 116, 2048−2058

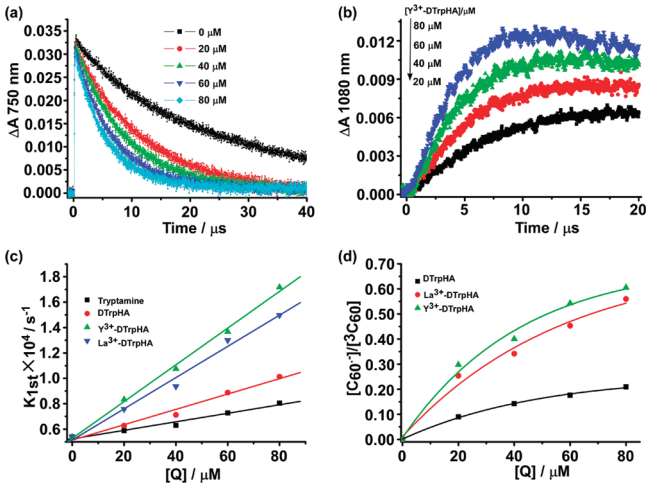

Figure 8. (a) Decay profiles of $^3C_{60}$ at 750 nm and (b) rising profile of $C_{60}^{\bullet-}$ at 1080 nm with changing [Y^{3+}–DTrpHA] in Ar-saturated DMSO–toluene (4/1, v/v) upon laser pulse (532 nm) irradiation. (c) Pseudo-first-order plot and (d) dependence of $[C_{60}^{\bullet-}]/[^3C_{60}*]$ on the concentration of DTrpHA, La^{3+}–DTrpHA, Y^{3+}–DTrpHA, or tryptamine.

1080 nm as follows (Figure 8d) (eq 6):[59]

$$[C_{60}^{\bullet-}]_{max}/[^3C_{60}*]_{max} = (\Delta A_{C_{60}^{\bullet-}}/\varepsilon_{C_{60}^{\bullet-}})/(\Delta A_{T_{C_{60}*}}/\varepsilon_{T_{C_{60}*}}) \quad (6)$$

where $\varepsilon_{C_{60}^{\bullet-}}$ (1.21×10^4 M^{-1} cm^{-1}) and $\varepsilon_{^3C_{60}*}$ (1.61×10^4 M^{-1} cm^{-1}) are the excitation coefficients of $C_{60}^{\bullet-}$ and $^3C_{60}*$, respectively.[60] The values of K_q^T and Φ_{ET}^T are summarized in Table 3 for C_{60} as triplet sensitizer and tryptamine,

Table 3. Rate Constants for Quenching (K_q^T) of $^3C_{60}*$, Quantum Yields (Φ_{ET}^T), and Rate Constants for Electron Transfer (K_{ET}^T) from Quenchers to $^3C_{60}*$

quenchers	K_q^T (M^{-1} s^{-1})	Φ_{ET}^T [a]	K_{ET}^T (M^{-1} s^{-1})
tryptamine	3.35×10^8	ND[b]	ND[b]
DTrpHA	6.05×10^8	0.208	1.26×10^8
La3+-DTrpHA	1.33×10^9	0.558	7.42×10^8
Y3+-DTrpHA	1.45×10^9	0.605	8.77×10^8

[a]Calculated when the quencher concentration is 80 μM. [b]ND means not detected.

DTrpHA, Y^{3+}–DTrpHA, and La^{3+}–DTrpHA as electron donor in DMSO–toluene solution, respectively.

Although $^3C_{60}*$ can be quenched by tryptamine efficiently (Figure 8c, Table 3), the transient absorbance peak of $C_{60}^{\bullet-}$ at 1080 nm cannot be detected in the tryptamine/C_{60} system, with the concentration of tryptamine in the range 20–80 μM. These results suggest the Φ_{ET}^T of tryptamine is quite lower than that of DTrpHA, Y^{3+}–DTrpHA or La^{3+}–DTrpHA. The K_q^T and Φ_{ET}^T values increase with their binding ability to C_{60} (Tables 2 and 3); i.e., the Φ_{ET}^T value for Y^{3+}–DTrpHA and La^{3+}–DTrpHA is larger than that of DTrpHA by a factor of 1.90 and 1.68, respectively.

The electron-transfer rate constant (K_{ET}^T) via $^3C_{60}*$ can be evaluated by the following equation (eq 7):

$$K_{ET}^T = K_q^T \times \Phi_{ET}^T \quad (7)$$

As shown in Table 3, K_{ET}^T values for Y^{3+}–DTrpHA and La^{3+}–DTrpHA are much larger than that of DTrpHA. That is because Y^{3+}–DTrpHA and La^{3+}–DTrpHA can form a stable supramolecular assembly with C_{60} ($K_a > 10^4$ M^{-1}, Table 2), ensuring efficient electron transfer from tryptamine in Y^{3+}–DTrpHA and La^{3+}–DTrpHA to $^3C_{60}*$. The K_q^T, K_{ET}^T, and Φ_{ET}^T values for Y^{3+}–DTrpHA and La^{3+}–DTrpHA are similar to that reported for the other electron donors, such as phthalocyanine, aromatic amine, and tetrathiafulvalene derivatives.[61]

The absorption band of ^3t-$BuC_{60}*$ at 720 nm and t-$BuC_{60}^{\bullet-}$ at 1020 nm[62] can be observed in the nanosecond transient absorption spectra of the Y^{3+}–DTrpHA/t-BuC_{60} assembly (Figure 9a). The decay curves of Y^{3+}–DTrpHA/t-BuC_{60} and

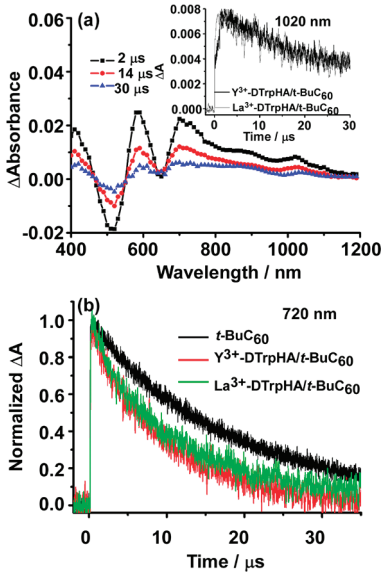

Figure 9. (a) Nanosecond transient absorption spectra of Y^{3+}–DTrpHA/t-BuC_{60} after 532 nm laser irradiation in Ar-saturated DMSO–toluene (4/1, v/v). (b) Time profiles of t-BuC_{60}, Y^{3+}–DTrpHA/t-BuC_{60}, and Y^{3+}–DTrpHA/t-BuC_{60} at 720 nm. Inset: Time profiles of Y^{3+}–DTrpHA/t-BuC_{60} and La^{3+}–DTrpHA/t-BuC_{60} at 1020 nm. [Y^{3+}–DtrpHA] = [La^{3+}–DtrpHA] = [t-BuC_{60}] = 40 μM.

La^{3+}–DTrpHA/t-BuC_{60} in the 720 nm system are fitted well with a double exponential function (faster and slower decay components) (Figure 9b). The faster components can be attributed to the interaction between M–DTrpHA and triplet t-BuC_{60} (Table S1, Supporting Information).

Similar to that of Y^{3+}–DTrpHA/t-BuC_{60}, the transient absorption spectrum of Y^{3+}–DTrpHA/MMC_{60} shows the absorption band of $^3MMC_{60}$ at 720 nm and $MMC_{60}^{\bullet-}$ at 1020 nm, indicating that photoinduced electron transfer between the tryptamine group and $^3MMC_{60}*$ occurs (Figure 10a). The decay rate of $^3MMC_{60}*$ increases after complexing with Y^{3+}–DTrpHA and La^{3+}–DTrpHA (Figure 10b). A shorter lifetime component was detected due to interaction between M–DTrpHA and MMC_{60} (Table S1, Supporting Information).

NIR Absorption Spectra. Spectroscopically, the fullerene C_{60} radical anion shows characteristic NIR absorption around 1080 nm. This band serves as a diagnostic probe for the identification of the one-electron reduced species. Upon irradiation of the solution of fullerene and tryptamine, no

dx.doi.org/10.1021/jp209969f | J. Phys. Chem. B 2012, 116, 2048–2058

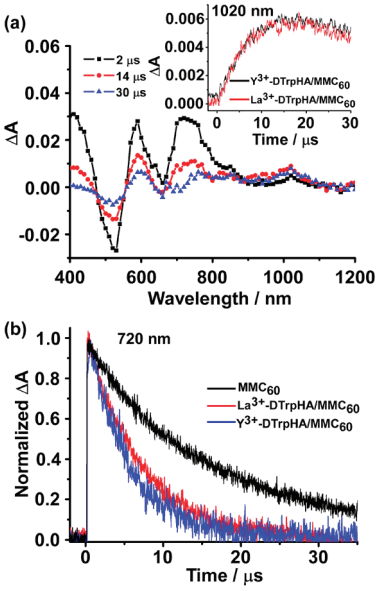

Figure 10. Nanosecond transient absorption spectra of Y^{3+}–DTrpHA/MMC_{60} after 532 nm laser irradiation in Ar-saturated DMSO–toluene (4/1, v/v). (b) Time profiles of MMC_{60}, Y^{3+}–DTrpHA/MMC_{60}, and La^{3+}–DTrpHA/MMC_{60} at 720 nm. Inset: Time profiles of Y^{3+}–DTrpHA/MMC_{60} and La^{3+}–DTrpHA/MMC_{60} at 1020 nm. [Y^{3+}–DtrpHA] = [La^{3+}–DtrpHA] = [MMC_{60}] = 40 μM.

NIR absorption band can be observed (Figure 11a). However, when fullerene is incubated with DTrpHA or Y^{3+}–DTrpHA

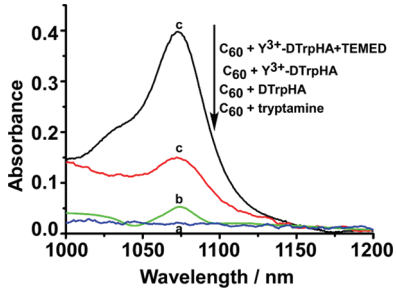

Figure 11. (a) NIR absorption spectra of argon-saturated DMSO–toluene (4/1, v/v) solution of C_{60} (40 μM) in the presence of (a) tryptamine (0.16 mM), (b) DTrpHA (80 μM), (c) Y^{3+}–DTrpHA (40 μM), and (d) Y^{3+}–DTrpHA (40 μM) and TEMED (1 mM), irradiated with a medium pressure sodium lamp for 5 min.

and then irradiated, a NIR absorption band at 1080 nm is observed (Figure 11b and c). With addition of a stronger reductant TEMED into the Y^{3+}–DTrpHA/C_{60} solution, the absorption band at 1080 nm increases obviously, further supporting that this band comes from one-electron reduction of C_{60} (Figure 11d). Considering that the concentration of tryptamine unit applied is the same in these cases, it can be deduced that electron transfer from tryptamine to fullerene in the Y^{3+}–DTrpHA/C_{60} or DTrpHA/C_{60} system is much more efficient than that in the simple mixture of fullerene and tryptamine, in consistence with the transient absorption results (Table 3). The fact that the intensity at 1080 nm in the Y^{3+}–DTrpHA/C_{60} system is stronger than that in DTrpHA/C_{60} can be attributed to the higher K_q^T, K_{ET}^T, and Φ_{ET}^T values for Y^{3+}–DTrpHA than those for DTrpHA during interaction with $^3C_{60}$* (Table 3). These phenomena may be due to the favorable spatial arrangement of donor–acceptor couples and thermodynamic feasibility of the electron-transfer processes in the supramolecular assembly.[63]

The photodynamics in the Y^{3+}–DTrpHA/C_{60} complex is summarized in Figure 12. The energy levels of the electron

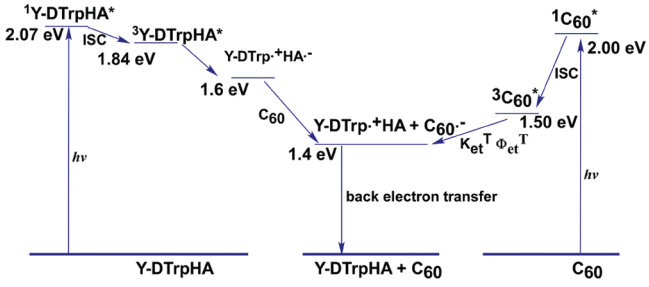

Figure 12. Schematic energy diagram for electron transfer in the Y^{3+}–DTrpHA/C_{60} system.

transfer processes can be estimated from the difference between the one-electron reduction potential of electron donors and the oxidation potential of the electron acceptors (Table 1). Photoexcitation of Y^{3+}–DTrpHA/C_{60} immediately affords both the singlet excited state of Y^{3+}–DTrpHA (2.07 eV)[64] and the singlet excited state of fullerene $^1C_{60}$* (2.00 eV).[65] These species undergo intersystem crossing (ISC) to give the triplet excited state of Y^{3+}–DTrpHA (1.84 eV) and triplet excited state of fullerene $^3C_{60}$* (1.50 eV), respectively. The intramolecular electron transfer in Y^{3+}–DTrpHA induces the generation of a charge-separated state Y^{3+}–$DTrp^{\bullet+}HA^{\bullet-}$, followed by electron transfer from Y^{3+}–$DTrp^{\bullet+}HA^{\bullet-}$ to C_{60},[20,30] forming the corresponding $C_{60}^{\bullet-}$. On the other hand, the intrasupramolecular electron transfer between Y^{3+}–DTrpHA and $^3C_{60}$* gives a charge separated state (Y^{3+}–$DTrp^{\bullet+}HA$ + $C_{60}^{\bullet-}$), which is the main pathway for the generation of $C_{60}^{\bullet-}$ according to the transient absorption results.

Transmission Electron Microscopy (TEM). The nanostructure of coordination polymer may be significantly affected by inclusion of guest molecules.[66] To further investigate the structure of the assemblies, transmission electron microscopy (TEM) experiments have been performed. Figure 13a indicates that Y^{3+}–DTrpHA may form a three-dimensional network, and the high solution TEM image suggests that Y^{3+}–DTrpHA displays an amorphous framework (Figure 13b). The TEM image of MMC_{60} shows particles with sizes of around 100 nm, which may be due to strong fullerene–fullerene interaction in polar solvents (Figure 13c and d).[67] The aggregation of MMC_{60} is remarkably reduced when forming a complex with Y^{3+}–DTrpHA (Figure 13e). The high resolution TEM image suggests that Y^{3+}–DTrpHA/MMC_{60} may form fiber-like structures with diameters of 15–30 nm (Figure 13f). Judging from the molecular scale of Y^{3+}–DTrpHA and MMC_{60}, it can be concluded that the self-assembled Y^{3+}–DTrpHA/MMC_{60} complex forms an interpenetrating network and large nanocluster.[68] Comparing the TEM images of Y^{3+}–DTrpHA before and after association with MMC_{60} (Figure 13b and f), the nanoscale structure of Y^{3+}–DTrpHA is rearranged upon inclusion of the guest molecule MMC_{60}.[66]

dx.doi.org/10.1021/jp209969f | J. Phys. Chem. B 2012, 116, 2048–2058

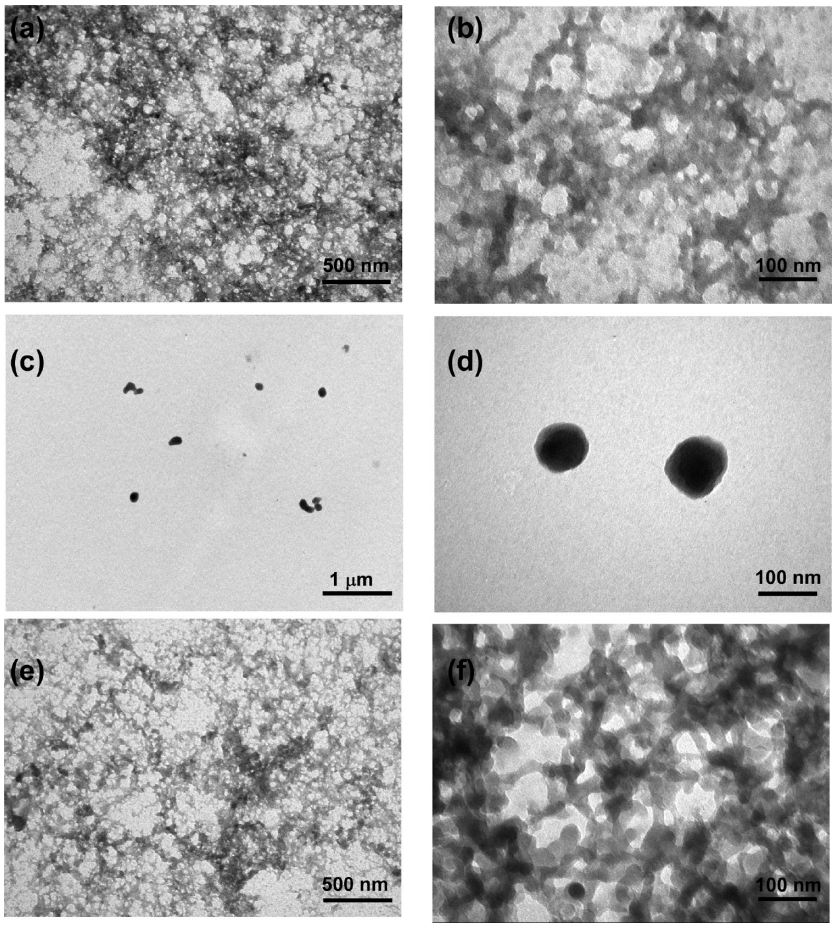

Figure 13. TEM images of Y^{3+}–DTrpHA (a, b), MMC_{60} (c, d), and Y^{3+}–DTrpHA/MMC_{60} (e, f) prepared in ethanol solution. [Y^{3+}–DTrpHA] = [MMC_{60}] = 100 μM.

CONCLUSIONS

In conclusion, we have synthesized two coordination polymers of tryptamine modified hypocrellin A, which can act as host molecules for fullerenes. The resulting M–DTrpHA/fullerene host–guest inclusion complexes can be stabilized through π–π stacking and electron donor–acceptor interactions. Electron transfer between the tryptamine motif in M–DTrpHA and fullerenes is enhanced upon formation of the supramolecular assembly, due to favorable spatial arrangement in confined nanospaces. The dynamic nanostructure of M–DTrpHA is significantly affected after being associated with fullerene.

ASSOCIATED CONTENT

Supporting Information

Supplementary transient absorption spectra, lifetimes of the transient intermediate, and general proceeding for preparation of DTrpHA and fullerene derivatives. This material is available free of charge via the Internet at http://pubs.acs.org.

AUTHOR INFORMATION

Corresponding Author

*E-mail: ouzhize@nwpu.edu.cn (Z.O.); gaoyunyan@nwpu.edu.cn (Y.G.). Phone/Fax: 86-29-88431677.

ACKNOWLEDGMENTS

This research is supported by National Natural Science Foundation of China (21073143), SRF for ROCS, SEM (N9YK0003, N9YK0005), and NPU Foundation for Fundamental Research (JC200822, JC20100239).

REFERENCES

(1) (a) Herm, Z. R.; Swisher, J. A.; Smit, B.; Krishna, R.; Long, J. R. *J. Am. Chem. Soc.* **2011**, *133*, 5664–5667. (b) Okubo, T.; Tanaka, N.; Kim, K. H.; Yone, H.; Maekawa, M.; Kuroda-Sowa, T. *Inorg. Chem.* **2010**, *49*, 3700–3702. (c) You, Y.; Yang, H.; Chung, J. W.; Kim, J. H.; Jung, Y.; Park, S. Y. *Angew. Chem., Int. Ed.* **2010**, *49*, 3757–3761. (d) Dan-Hardi, M.; Serre, C.; Frot, T.; Rozes, L.; Maurin, G.; Sanchez, C.; Ferey, G. *J. Am. Chem. Soc.* **2009**, *131*, 10857–10859. (e) Spokoyny, A. M.; Kim, D.; Sumrein, A.; Mirkin, C. A. *Chem. Soc. Rev.* **2009**, *38*, 1218–1227.

(2) (a) Lee, S. Y.; Lee, S. S. *CrystEngComm* **2010**, *12*, 3471–3475. (b) Wheaton, C. A.; Jennings, M. C.; Puddephatt., R. J. *J. Am. Chem. Soc.* **2006**, *128*, 15370–15371.

(3) (a) Yaghi, O. M.; O'Keeffe, M.; Ockwig, N. W.; Chae, H. K.; Eddaoudi, M.; Kim, J. *Nature* **2003**, *423*, 705–714. (b) Ferey, G.; Mellot-Dranznieks, C.; Serre, C.; Millange, F. *Acc. Chem. Res.* **2005**, *38*, 217–225.

(4) (a) Xing, Y.; Lin, J.; Xu, Y.; Duan, X.; Li, Y.; Wang, F.; Meng, Q. *Inorg. Chem. Commun.* **2010**, *13*, 514–517. (b) Uemura, K.; Saito, K.; Kitagawa, S.; Kita, H. *J. Am. Chem. Soc.* **2006**, *128*, 16122–16130.

(5) (a) Zhang, X.; Ballem, M. A.; Ahren, M.; Suska, A.; Bergman, P.; Uvdal, K. *J. Am. Chem. Soc.* **2010**, *132*, 10391–10397. (b) Cui, H. B.; Zhou, B.; Long, L. S.; Yoshinori, O.; Kobayashi, H.; Kobayashi, A. *Angew. Chem., Int. Ed.* **2008**, *47*, 3376–3380.

(6) (a) Sapchenko, S. A.; Samsonenko, D. G.; Dybtsev, D. N.; Melgunov, M. S.; Fedin, V. P. *Dalton Trans.* **2011**, *40*, 2196–2203.

(b) Ono, K.; Klosterman, J. K.; Yoshizawa, M.; Sekiguchi, K.; Tahara, T.; Fujita, M. *J. Am. Chem. Soc.* **2009**, *131*, 12526−12527.
(7) (a) Shimomura, S.; Kitagawa, S. *J. Mater. Chem.* **2011**, *21*, 5537−5546. (b) Dybtsev, D. N.; Yutkin, M. P.; Samsonenko, D. G.; Fedin, V. P.; Nuzhdin, A. L.; Bezrukov, A. A.; Bryliakov, K. P.; Talsi, E. P.; Belosludov, R. V.; Mizuseki, H.; Kawazoe, Y.; Subbotin, O. S.; Belosludov, V. R. *Chem.—Eur. J.* **2010**, *16*, 10348−10356.
(8) (a) Pramanik, S.; Zheng, C.; Zhang, X.; Emge, T. J.; Li, J. *J. Am. Chem. Soc.* **2011**, *133*, 4153−4155. (b) Zheng, G.; Zhang, H. J.; Song, S. Y.; Li, Y. Y.; Guo, H. D. *Eur. J. Inorg. Chem.* **2008**, 17561759. (c) Pai, C. H.; Hasegawa, S.; Horike, S.; Matsuda, R.; Furukawa, S.; Mochizuki, K.; Kinoshita, Y.; Kitagawa, S. *J. Am. Chem. Soc.* **2007**, *129*, 2607−2614.
(9) (a) Guldi, D. M.; Luo, C.; Kotov, N. A.; Da Ros, T.; Bosi, S.; Prato, M. *J. Phys. Chem. B* **2003**, *107*, 7293−7298. (b) Imahori, H.; Hagiwara, K.; Aoki, M.; Akiyama, T.; Taniguchi, S.; Okada, T.; Shirakawa, M.; Sakata, Y. *J. Am. Chem. Soc.* **1996**, *118*, 11771−11782.
(10) MacLeod, J. M.; Ivasenko, O.; Fu, C.; Taerum, T.; Rosei, F.; Perepichka, D. F. *J. Am. Chem. Soc.* **2009**, *131*, 16844−16850.
(11) Megiatto, J. D. Jr.; Schuster, D. I.; Abwandner, S.; de Miguel, G.; Guldi, D. M. *J. Am. Chem. Soc.* **2010**, *132*, 3847−3861.
(12) (a) Grimm, B.; Schornbaum, J.; Cardona, C. M.; Van Paauwe, J. D.; Boyd, P. D. W.; Guldi, D. M. *Chem. Sci.* **2011**, *2*, 1530−1537. (b) Haino, T.; Hirai, E.; Fujiwara, Y.; Kashihara, K. *Angew. Chem., Int. Ed.* **2010**, *49*, 7899−7903. (c) Tian, X. H.; Chen, C. F. *Chem.—Eur. J.* **2010**, *16*, 8072−8079.
(13) Huerta, E.; Isla, H.; Perez, E. M.; Bo, C.; Martin, N.; De Mendoza, J. *J. Am. Chem. Soc.* **2010**, *132*, 5351−5353.
(14) Iwamoto, T.; Watanabe, Y.; Sadahiro, T.; Haino, T.; Yamago, S. *Angew. Chem.* **2011**, *123*, 8492−8494.
(15) Canevet, D.; Gallego, M.; Isla, H.; De Juan, A.; Perez, E. M.; Martin, N. *J. Am. Chem. Soc.* **2011**, *133*, 3184−3190.
(16) (a) Hernandez-Eguia, L. P.; Escudero-Adan, E. C.; Pinzon, J. R.; Echegoyen, L.; Ballester, P. *J. Org. Chem.* **2011**, *76*, 3258−3265. (b) Nobukuni, H.; Shimazaki, Y.; Uno, H.; Naruta, Y.; Ohkubo, K.; Kojima, T.; Fukuzumi, S.; Seki, S.; Sakai, H.; Hasobe, T.; Tani, F. *Chem.—Eur. J.* **2010**, *16*, 11611−11623.
(17) (a) Meng, W.; Breiner, B.; Rissanen, K.; Thoburn, J. D.; Clegg, J. K.; Nitschke, J. R. *Angew. Chem.* **2011**, *123*, 3541−3545. (b) Constable, E. C.; Zhang, G.; Haussinger, D.; Housecroft, C. E.; Zampese, J. A. *J. Am. Chem. Soc.* **2011**, *133*, 10776−10779. (c) Kishi, N.; Li, Z.; Yoza, K.; Akita, M.; Yoshizawa, M. *J. Am. Chem. Soc.* **2011**, *133*, 11438−11441.
(18) (a) Inokuma, Y.; Arai, T.; Fujita, M. *Nat. Chem.* **2010**, *2*, 780−783. (b) Konarev, D. V.; Khasanov, S. S.; Kovalevsky, A. Y.; Lopatin, D. V.; Rodaev, V. V.; Saito, G.; Nafradi, B.; Forro, L.; Lyubovskaya, R. N. *Cryst. Growth Des.* **2008**, *8*, 1161−1172. (c) Sun, D.; Tham, F. S.; Reed, C. A.; Boyd, P. D. W. *Proc. Natl. Acad. Sci. U.S.A.* **2002**, *99*, 5088−5092. (d) Sharma, C. V. K.; Broker, G. A.; Huddleston, J. G.; Baldwin, J. W.; Metzger, R. M.; Rogers, R. D. *J. Am. Chem. Soc.* **1999**, *121*, 1137−1141.
(19) Uyar, Z.; Satake, A.; Kobuke, Y.; Hirota, S. *Tetrahedron Lett.* **2008**, *49*, 5484−5487.
(20) Ou, Z.; Guo, C.; Gao, Y.; Li, S.; Yin, W.; Li, Y.; Jin, M.; Wang, X.; Yang, G. *J. Photochem. Photobiol., A* **2011**, *217*, 228−235.
(21) Gao, Y.; Ou, Z.; Zhang, Z.; Li, S.; Yang, G.; Wang, X. *Acta Phys. Chim. Sin.* **2009**, *25*, 74−78.
(22) (a) Ling, K. Q.; Li, W. S.; Sayre, L. M. *J. Am. Chem. Soc.* **2008**, *130*, 933−944. (b) Hibino, S.; Choshi, T. *Nat. Prod. Rep.* **2001**, *18*, 66−87.
(23) Rossi, E.; Van de Vorst, A.; Jori, G. *Photochem. Photobiol.* **1981**, *34*, 447−454.
(24) (a) Zeng, Z.; Zhou, J.; Zhang, Y.; Qiao, R.; Xia, S.; Chen, J.; Wang, X.; Zhang, B. *J. Phys. Chem. B* **2007**, *111*, 2688−2696. (b) Zhou, J. H.; Liu, J. H.; Xia, S. Q.; Chen, J. R.; Wang, X. S.; Zhang, B. W. *J. Phys. Chem. B* **2005**, *109*, 19529−19535.
(25) Okamoto, K.; Araki, Y.; Ito, O.; Fukuzumi, S. *J. Am. Chem. Soc.* **2004**, *126*, 56−57.
(26) (a) Takai, A.; Chkounda, M.; Eggenspiller, A.; Gros, C. P.; Lachkar, M.; Barbe, J. M.; Fukuzumi, S. *J. Am. Chem. Soc.* **2010**, *132*, 4477−4489. (b) D'Souza, F.; Chitta, R.; Gadde, S.; Zandler, M. E.; Sandanayaka, A. S. D.; Araki, Y.; Ito, O. *Chem. Commun.* **2005**, 1279−1281.
(27) Zhang, L.; Chen, J.; Li, S.; Chen, J.; Li, Y.; Yang, G.; Li, Y. *J. Photochem. Photobiol., A* **2006**, *181*, 429−436.
(28) Li, Y.; Dini, D.; Calvete, M. J. F.; Hanack, M.; Sun, W. *J. Phys. Chem. A* **2008**, *112*, 472−480.
(29) Dubois, D.; Kadish, K. M.; Flanagan, S.; Haufler, R. E.; Chibante, L. P. F; Wilson, L. J. *J. Am. Chem. Soc.* **1991**, *113*, 4364−4366.
(30) Gao, Y.; Ou, Z.; Chen, J.; Yang, G.; Wang, X.; Zhang, B.; Jin, M.; Liu, L. *New J. Chem.* **2008**, *32*, 1555−1560.
(31) Inoue, Y.; Yamamoto, K.; Wada, T.; Everitt, S.; Gao, X.; Hou, Z.; Tong, L.; Jiang, S.; Wu, H. *J. Chem. Soc., Perkin Trans.* **1998**, *2*, 1807−1816.
(32) (a) Liu, Y.; Zhou, Q.; Zeng, Z.; Qiao, R.; Wang, X.; Zhang, B. *J. Phys. Chem. B* **2008**, *112*, 9959−9965. (b) Xia, S. Q.; Zhou, J. H.; Chen, J. R.; Wang, X.; Zhang, B. W. *Chem. Commun.* **2003**, 1372−1373. (c) Ou, Z.; Chen, J.; Wang, X.; Zhang, B.; Cao, Y. *New J. Chem.* **2002**, *26*, 1130−1136. (d) He, Y. Y.; An, J. Y.; Zou, W.; Jiang, L. J. *J. Photochem. Photobiol., B* **1998**, *44*, 45−52.
(33) Jovanovic, S. V.; Harriman, A.; Simic, M. G. *J. Phys. Chem.* **1986**, *90*, 1935−1939.
(34) Harvey, A. E. Jr.; Manning, D. L. *J. Am. Chem. Soc.* **1950**, *72*, 4488−4493.
(35) DelMedico, A.; Pietro, W. J.; Lever, A. B. P. *Inorg. Chim. Acta* **1998**, *281*, 126−133.
(36) Wan, Y.; Zhang, L.; Jin, L.; Gao, S.; Lu, S. *Inorg. Chem.* **2003**, *42*, 4985−4994.
(37) (a) Wan, Y. H.; Jin, L. P.; Wang, K. Z.; Zhang, L. P.; Zheng, X. Z.; Lu, S. Z. *New J. Chem.* **2002**, *26*, 1590−1596. (b) Lewinski, J.; Dranka, M.; Bury, W.; Saliwinski, W.; Justyniak, I.; Lipkowski, J. *J. Am. Chem. Soc.* **2007**, *129*, 3096−3098. (c) Maji, T. K.; Ohba, M.; Kitagawa, S. *Inorg. Chem.* **2005**, *44*, 9225−9231.
(38) (a) Martin, N.; Sanchez, L.; Illescas, B.; Perez, I. *Chem. Rev.* **1998**, *98*, 2527−2547. (b) Weng, M.; Zhang, M. H.; Wang, W. Q.; Shen, T. *J. Chem. Soc., Faraday Trans.* **1997**, *93*, 3491−3495.
(39) Yin, W.; Ou, Z.; Gao, Y.; Hao, P.; Guo, C.; Wang, Z. *Acta Chim. Sin.* **2010**, *14*, 1343−1348.
(40) Rehm, D.; Weller, A. *Isr. J. Chem.* **1970**, *7*, 259−271.
(41) Keshavarz-K, M.; Knight, B.; Haddon, R. C.; Wudl, F. *Tetrahedron* **1996**, *52*, 5149−5159.
(42) Guldi, D. M.; Prato, M. *Acc. Chem. Res.* **2000**, *33*, 695−703.
(43) (a) De La Escosura, A.; Martinez-Diaz, M. V.; Guldi, D. M.; Torres, T. *J. Am. Chem. Soc.* **2006**, *128*, 4112−4118. (b) D'Souza, F.; Ito, O. *Chem. Commun.* **2009**, 4913−4928.
(44) Tashiro, K.; Aida, T. *Chem. Soc. Rev.* **2007**, *36*, 189−197.
(45) Liu, Y.; Yang, Z. X.; Chen, Y.; Song, Y.; Shao, N. *ACS Nano* **2008**, *2*, 554−560.
(46) Liu, Y.; Wang, H.; Chen, Y.; Ke, C.; Liu, M. *J. Am. Chem. Soc.* **2005**, *127*, 657−666.
(47) Petrich, J. W.; Longworth, J. W.; Fleming, G. R. *Biochemistry* **1987**, *26*, 2711−2722.
(48) Zheng, J. Y.; Tashiro, K.; Hirabayashi, Y.; Kinbara, K.; Saigo, K.; Aida, T.; Sakamoto, S.; Yamaguchi, K. *Angew. Chem., Int. Ed.* **2001**, *40*, 1857−1861.
(49) Haino, T.; Matsumoto, Y.; Fukazawa, Y. *J. Am. Chem. Soc.* **2005**, *127*, 8936−8937.
(50) (a) Wessendorf, F.; Gnichwitz, J. F.; Sarova, G. H.; Hager, K.; Hartnagel, U.; Guldi, D. M.; Hirsch, A. *J. Am. Chem. Soc.* **2007**, *129*, 16057−16071. (b) Mateo-Alonso, A.; Sooambar, C.; Prato, M. *Org. Biomol. Chem.* **2006**, *4*, 1629−1637. (c) Innocenzi, P.; Brusatin, G. *Chem. Mater.* **2001**, *13*, 3126−3139. (d) Yanase, M.; Matsuoka, M.; Tatsumi, Y.; Suzuki, M.; Iwamoto, H.; Haino, T.; Fukazawa, Y. *Tetrahedron Lett.* **2000**, *41*, 493−497.

(51) (a) Muniappan, S.; Lipstman, S.; George, S.; Goldberg, I. *Inorg. Chem.* **2007**, *46*, 5544−5554. (b) Rogers, R. D.; Etzenhouser, R. D.; Murdoch, J. S.; Reyes, E. *Inorg. Chem.* **1991**, *30*, 1445−1455.
(52) Dimos, A.; Tsaousis, D.; Michaelides, A.; Skoulika, S.; Golhen, S.; Ouahab, L.; Didierjean, C.; Aubry, A. *Chem. Mater.* **2002**, *14*, 2616−2622.
(53) Pitzer, K. S. *Acc. Chem. Res.* **1979**, *12*, 271−276.
(54) Leland, B. A.; Joran, A. D.; Felker, P. M.; Hopfield, J. J.; Zewail, A. H.; Dervan, P. B. *J. Phys. Chem.* **1985**, *89*, 5571−5573. (b) Wasielewski, M. R. *Chem. Rev.* **1992**, *92*, 435−461.
(55) Wagenknecht, H. A.; Stemp, Eric D. A.; Barton, J. K. *J. Am. Chem. Soc.* **2000**, *122*, 1−7.
(56) Nonell, S.; Arbogast, J. W.; Foote, C. S. *J. Phys. Chem.* **1992**, *96*, 4169−4170.
(57) Guldi, D. M.; Hungerbuehler, H.; Janata, E.; Asmus, K. D. *J. Chem. Soc., Chem. Commun.* **1993**, 84−86.
(58) Alam, M. M.; Watanabe, A.; Ito, O. *J. Photochem. Photobiol., A* **1997**, *104*, 59−64.
(59) Andrews, L. J.; Levy, J. M.; Linschitz, H. *J. Photochem.* **1977**, *6*, 355−364.
(60) (a) Arbogast, J. W.; Darmanyan, A. P.; Foote, C. S.; Rubin, Y.; Diederich, F. N.; Alvarez, M. M.; Anz, S. J.; Whetten, R. L. *J. Phys. Chem.* **1991**, *95*, 11−12. (b) Heath, G. A.; McGrady, J. E.; Martin, R. L. *J. Chem. Soc., Chem. Commun.* **1992**, 1272−1274.
(61) (a) Alam, M. M.; Watanabe, A.; Ito, O. *J. Photochem. Photobiol., A* **1997**, *104*, 59−64. (b) Sasaki, Y.; Araki, Y.; Ito, O.; Alam, M. M. *Photochem. Photobiol. Sci.* **2007**, *6*, 560−565. (c) Nojiri, T.; Alam, M. M.; Konami, H.; Watanabe, A.; Ito, O. *J. Phys. Chem. A* **1997**, *101*, 7943−7947.
(62) Araki, Y.; Chitta, R.; Sandanayaka, A. S. D.; Langenwalter, K.; Gadde, S.; Zandler, M. E.; Ito, O.; D'Souza, F. *J. Phys. Chem. C* **2008**, *112*, 2222−2229.
(63) (a) Garg, V.; Kodis, G.; Chachisvilis, M.; Hambourger, M.; Moore, A. L.; Moore, T. A.; Gust, D. *J. Am. Chem. Soc.* **2011**, *133*, 2944−2954. (b) Chitta, R.; D'Souza, F. *J. Mater. Chem.* **2008**, *18*, 1440−1471.
(64) Zhang, M.; Weng, M.; Chen, S.; Xia, W.; Jiang, L.; Chen, D. *J. Photochem. Photobiol., A* **1996**, *96*, 57−63.
(65) Nobukuni, H.; Shimazaki, Y.; Uno, H.; Naruta, Y.; Ohkubo, K.; Kojima, T.; Fukuzumi, S.; Seki, S.; Sakai, H.; Hasobe, T.; Tani, F. *Chem.—Eur. J.* **2010**, *16*, 11611−11623.
(66) Tanaka, D.; Kitagawa, S. *Chem. Mater.* **2008**, *20*, 922−931.
(67) Nath, S.; Pal, H.; Sapre, A. V. *Chem. Phys. Lett.* **2002**, *360*, 422−428.
(68) (a) Saito, K.; Troiani, V.; Qiu, H. *J. Phys. Chem. C* **2007**, *111*, 1194−1199. (b) Hasobe, T.; Saito, K.; Kamat, P. V. *J. Mater. Chem.* **2007**, *17*, 4160−4170.